



Tunneling-injection of electrons and holes into quantum dots: A tool for high-power lasing

Dae-Seob Han and Levon V. Asryan

Citation: [Applied Physics Letters](#) **92**, 251113 (2008); doi: 10.1063/1.2952488

View online: <http://dx.doi.org/10.1063/1.2952488>

View Table of Contents: <http://scitation.aip.org/content/aip/journal/apl/92/25?ver=pdfcov>

Published by the [AIP Publishing](#)

Articles you may be interested in

[High performance tunnel injection quantum dot comb laser](#)

Appl. Phys. Lett. **96**, 101107 (2010); 10.1063/1.3358142

[Experimental demonstration of the polarization-dependent photon-mediated carrier redistribution in tunneling injection InP quantum-dot lasers with external-grating feedback](#)

Appl. Phys. Lett. **90**, 211102 (2007); 10.1063/1.2741118

[Subpicosecond high-power mode locking using flared waveguide monolithic quantum-dot lasers](#)

Appl. Phys. Lett. **88**, 133119 (2006); 10.1063/1.2186110

[Electron-hole asymmetry and two-state lasing in quantum dot lasers](#)

Appl. Phys. Lett. **87**, 053113 (2005); 10.1063/1.1995947

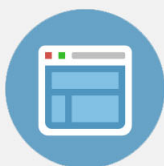
[High-speed 1.3 \$\mu\$ m tunnel injection quantum-dot lasers](#)

Appl. Phys. Lett. **86**, 153109 (2005); 10.1063/1.1899230



Re-register for Table of Content Alerts

Create a profile.



Sign up today!



Tunneling-injection of electrons and holes into quantum dots: A tool for high-power lasing

Dae-Seob Han and Levon V. Asryan^{a)}

Virginia Polytechnic Institute and State University, Blacksburg, Virginia 24061, USA

(Received 8 March 2008; accepted 6 June 2008; published online 26 June 2008)

We study the optical output power of a semiconductor laser, which exploits tunneling-injection of electrons and holes into quantum dots (QDs) from two separate quantum wells. Even if there is out-tunneling leakage of carriers from QDs, the intensity of parasitic recombination outside QDs remains restricted with increasing injection current. As a result, the light-current characteristic becomes increasingly linear, and the slope efficiency grows closer to unity at high injection currents—a fascinating feature favoring the use of tunneling-injection of both electrons and holes into QDs for high-power lasing. © 2008 American Institute of Physics. [DOI: 10.1063/1.2952488]

In the conventional design of quantum dot (QD) lasers, the conductive optical confinement layer (OCL) transports mobile carriers to the QDs. Due to bipolar population in the OCL, a certain fraction of the injection current goes into the electron-hole recombination there. The parasitic recombination outside QDs is a major source of temperature dependence of the threshold current. The carrier capture from the OCL into QDs is not instantaneous. For this reason, the carrier density in the OCL and hence the parasitic recombination rate rise, even above the lasing threshold, with injection current. This leads to sublinearity of the light-current characteristic (LCC) and limits the output power.¹ Suppression of the parasitic recombination would be expected to significantly enhance the temperature stability and the output optical power of a laser.

Several approaches have been proposed to improve QD laser characteristics. Among them are *p*-type modulation doping of the active region^{2,3} and tunneling-injection into QDs. In Refs. 4–6, to minimize hot carrier effects, tunneling-injection of only electrons into QDs was proposed from a single quantum well (QW) (previously, tunneling-injection into the QW was utilized with the same purpose in a QW laser⁷). In the structures of Refs. 4–6, bipolar carrier density and hence parasitic recombination still remain on the hole-injecting side. In Ref. 8, resonant tunneling was proposed from the bulk region (OCL) into the QD excited state.

In Refs. 9–11, to suppress the recombination outside QDs and thus to improve the temperature-stability of the laser, tunneling-injection of both electrons and holes into QDs was proposed from two separate QWs. There have been recent experimental developments^{12–15} related to this concept.

Compared to a conventional QD laser, tunneling-injection can efficiently improve the uniformity of QDs by selecting the QDs of the “right” size;^{9–12} the carrier collection in QDs can also be improved.¹² Using tunneling-injection of both electrons and holes, the highest reported ground-state gain for a single-layer InAs QD laser was achieved, thus allowing for ground-state lasing in short-cavity devices.¹³ A more symmetrical gain shape and a smaller refractive index change at the peak gain wavelength

were reported for a tunneling-injection laser.¹⁵

Here, we study the potential of tunneling-injection of both electrons and holes into QDs for high-power operation and develop an extended model for a realistic device. The energy band diagram of the structure is shown in Fig. 1. A single layer with QDs is clad on each side by a QW separated from the QDs by a thin barrier. Electrons (holes) are injected into QDs by tunneling from the left (right)-hand-side QW. The key idea of the device is that the QWs are not connected by a current path that bypasses QDs. Figure 1 shows the most optimum situation, when the lowest subband edge for majority carriers in the QW is in resonance with the energy level for the corresponding type of carrier in the average-sized QD, and hence the tunneling-injection rate is at its maximum. Tunneling-injection does not necessarily have to occur into the QD ground state. Carriers can efficiently tunnel from the QW to the QD excited state, and then relax rapidly to the QD ground state for stimulated recombination.^{16,17} In Refs. 13 and 15, lasing action from the QD excited state was reported.

In an ideal situation, there is no second tunneling step, i.e., out-tunneling from QDs into the “foreign” QWs

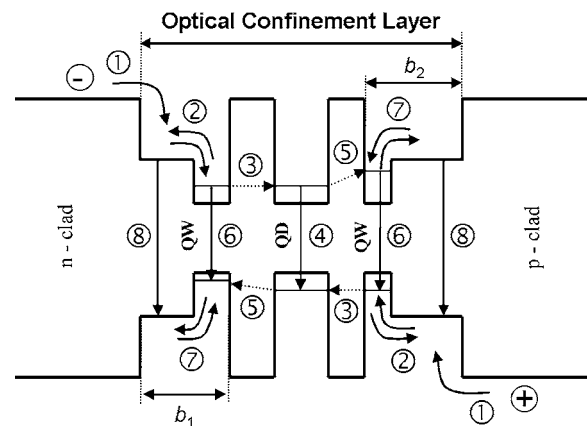


FIG. 1. Energy band diagram of a tunneling-injection QD laser and the main processes: ① carrier injection from the cladding layers to the OCL, ② majority carrier capture from the OCL into the QW and thermal escape from the QW to the OCL, ③ carrier tunneling from the QW into a QD, ④ spontaneous and stimulated recombination in a QD, ⑤ carrier out-tunneling from a QD into the foreign QW, ⑥ spontaneous recombination in the QWs, ⑦ minority carrier thermal escape from the QW to the OCL and capture from the OCL into the QW, and ⑧ spontaneous recombination in the OCL.

^{a)}Electronic mail: asryan@mse.vt.edu. URL: <http://www.mse.vt.edu/people/faculty/asryan.html>.

(electron-injecting QW for holes, and hole-injecting QW for electrons). Accordingly, there will be no electrons (holes) in the hole (electron)-injecting side of the structure. As shown below, the total suppression of bipolar population and, consequently, of recombination outside QDs leads to an ideal LCC.

Out-tunneling into the foreign QWs cannot be completely blocked in actual devices. Figure 1 shows an optimized structure, in which the lowest subband edge for minority carriers in the QW is misaligned from the energy level for the corresponding type of carrier in the QD. Even in such a structure, there will be an indirect out-tunneling (shown by the inclined arrows in Fig. 1)—electrons (holes) as minority carriers will appear in the hole (electron)-injecting QW. Then they will thermally escape to the right (left)-hand side of the OCL where holes (electrons) are the majority carriers. As a result, a bipolar population will establish outside QDs, and parasitic recombination will occur. Our model includes these processes and is based on the following set of rate equations:

$$b_1 \frac{\partial n_L}{\partial t} = \frac{j}{e} + \frac{n_{\text{QW}}^L}{\tau_{n,\text{esc}}^L} - v_{n,\text{capt}}^L n_L - b_1 B n_L p_L, \quad (1)$$

$$b_1 \frac{\partial p_L}{\partial t} = \frac{p_{\text{QW}}^L}{\tau_{p,\text{esc}}^L} - v_{p,\text{capt}}^L p_L - b_1 B n_L p_L, \quad (2)$$

$$\begin{aligned} \frac{\partial n_{\text{QW}}^L}{\partial t} &= v_{n,\text{capt}}^L n_L - \frac{n_{\text{QW}}^L}{\tau_{n,\text{esc}}^L} - w_{n,\text{tunn}}^L N_S (1 - f_n) n_{\text{QW}}^L \\ &\quad + w_{n,\text{tunn}}^L n_1^{L,\text{QW}} N_S f_n - B_{2\text{D}} n_{\text{QW}}^L p_{\text{QW}}^L, \end{aligned} \quad (3)$$

$$\begin{aligned} \frac{\partial p_{\text{QW}}^L}{\partial t} &= v_{p,\text{capt}}^L p_L - \frac{p_{\text{QW}}^L}{\tau_{p,\text{esc}}^L} - w_{p,\text{tunn}}^L N_S (1 - f_p) p_{\text{QW}}^L \\ &\quad + w_{p,\text{tunn}}^L n_1^{L,\text{QW}} N_S f_p - B_{2\text{D}} n_{\text{QW}}^L p_{\text{QW}}^L, \end{aligned} \quad (4)$$

$$\begin{aligned} N_S \frac{\partial f_n}{\partial t} &= w_{n,\text{tunn}}^L N_S (1 - f_n) n_{\text{QW}}^L - w_{n,\text{tunn}}^L n_1^{L,\text{QW}} N_S f_n \\ &\quad + w_{n,\text{tunn}}^R N_S (1 - f_n) n_{\text{QW}}^R - w_{n,\text{tunn}}^R n_1^{R,\text{QW}} N_S f_n \\ &\quad - N_S \frac{f_n f_p}{\tau_{\text{QD}}} - \frac{c}{\sqrt{\epsilon_g}} \frac{g^{\text{max}}}{S} (f_n + f_p - 1) N, \end{aligned} \quad (5)$$

$$\frac{\partial N}{\partial t} = \frac{c}{\sqrt{\epsilon_g}} g^{\text{max}} (f_n + f_p - 1) N - \frac{c}{\sqrt{\epsilon_g}} \beta N. \quad (6)$$

The equation for holes confined in QDs is similar to Eq. (5), and the equations for carriers in the right-hand-side QW and OCL are similar to Eqs. (1)–(4).

In Eqs. (1)–(6), b_1 is the thickness of the left-hand side of the OCL and n_L and p_L are the free-electron and free-hole densities there (Fig. 1), j is the injection current density, e is the electron charge, n_{QW}^L and p_{QW}^L are the two-dimensional (2D) electron and hole densities in the left-hand-side QW (Fig. 1), B and $B_{2\text{D}}$ are the spontaneous radiative recombination constants for the bulk (OCL) and 2D region (QWs), respectively, N_S is the surface density of QDs, $f_{n,p}$ are the electron- and hole-level occupancies in QDs, τ_{QD} is the spontaneous radiative lifetime in a QD, c is the velocity of light in vacuum, $\sqrt{\epsilon_g}$ is the group index of the dispersive OCL material, g^{max} is the maximum value of the modal gain,¹⁸ S is the cross section of the junction, N is the number of photons in

the lasing mode, and β is the mirror loss; $\tau_{n,p,\text{esc}}^{L,R}$ are the thermal escape times of electrons and holes from the QWs to the OCL and $v_{n,p,\text{capt}}^{L,R}$ are the capture velocities from the OCL to the QWs.

We exploit four tunneling coefficients, $w_{n,p,\text{tunn}}^{L,R}$ (measured in units of cm^2/s), for electron and hole tunneling between the QD ensemble and the QWs. The quantities $n_1^{L,R,\text{QW}}$ and $p_1^{L,R,\text{QW}}$ in the electron and hole tunneling fluxes from the QD ensemble to the QWs [see Eqs. (3)–(5)] are related to the 2D effective densities of states in the conduction and valence bands in the QWs.

In Eqs. (3) and (5), $w_{n,\text{tunn}}^L N_S (1 - f_n) n_{\text{QW}}^L - w_{n,\text{tunn}}^L n_1^{L,\text{QW}} N_S f_n$ is the net in-tunneling flux of electrons from the electron-injecting QW into QDs. In Eq. (4), $w_{p,\text{tunn}}^L p_1^{L,\text{QW}} N_S f_p - w_{p,\text{tunn}}^L N_S (1 - f_p) p_{\text{QW}}^L$ is the net out-tunneling flux of holes from QDs to the electron-injecting QW.

We consider a continuous-wave operation and correspondingly use the rate equations at the steady state ($\partial/\partial t = 0$). In terms of the excess of the injection current density over the current densities of the spontaneous recombination in QDs, QWs, and OCL, the output power is

$$\begin{aligned} P &= \frac{\hbar\omega}{e} S \left(j - e N_S \frac{f_n f_p}{\tau_{\text{QD}}} - e B_{2\text{D}} n_{\text{QW}}^L p_{\text{QW}}^L - e B_{2\text{D}} n_{\text{QW}}^R p_{\text{QW}}^R \right. \\ &\quad \left. - e b_1 B n_L p_L - e b_2 B n_R p_R \right). \end{aligned} \quad (7)$$

If out-tunneling into the foreign QWs is completely blocked ($w_{p,\text{tunn}}^L, w_{n,\text{tunn}}^R = 0$), there will be no minority carriers outside QDs ($p_L, p_{\text{QW}}^L, n_{\text{QW}}^R, n_R = 0$). The electron-hole recombination will occur only in QDs. Equation (7) will read as

$$P^{\text{highest}} = \frac{\hbar\omega}{e} S \left(j - e N_S \frac{f_n f_p}{\tau_{\text{QD}}} \right). \quad (8)$$

The level occupancies $f_{n,p}$ cannot exceed unity; hence, the spontaneous recombination current density in QDs, $e N_S (f_n f_p / \tau_{\text{QD}})$, cannot exceed $e N_S / \tau_{\text{QD}}$. For typical values of N_S (below 10^{11} cm^{-2}) and τ_{QD} (around 1 ns), $e N_S / \tau_{\text{QD}}$ is less than 20 A/cm^2 . This means that for $j > 100 \text{ A/cm}^2$, the spontaneous recombination term can be safely neglected compared to j in Eq. (8). As a result, the LCC of an ideal tunneling-injection QD laser is virtually linear and the slope efficiency, $\eta_{\text{ext}} = (e/\hbar\omega)(1/S)\partial P/\partial j$, is unity. The reason is that the only remaining channel of nonstimulated recombination in this case is the spontaneous recombination in QDs, which is weak.

In an actual structure, there can be out-tunneling into the foreign QWs (Fig. 1). For this reason, the electron-hole recombination outside QDs cannot be completely suppressed. Hence, the rate equations should be solved in the general case of nonvanishing tunneling coefficients $w_{p,\text{tunn}}^L$ and $w_{n,\text{tunn}}^R$. From Eqs. (2) and (4) at the steady state, we have

$$\begin{aligned} B_{2\text{D}} n_{\text{QW}}^L p_{\text{QW}}^L + b_1 B n_L p_L \\ = w_{p,\text{tunn}}^L p_1^{L,\text{QW}} N_S f_p - w_{p,\text{tunn}}^L N_S (1 - f_p) p_{\text{QW}}^L. \end{aligned} \quad (9)$$

As seen from Eq. (9), bimolecular recombination in the left-hand-side QW and OCL is entirely due to the net out-tunneling of holes from QDs to the QW.

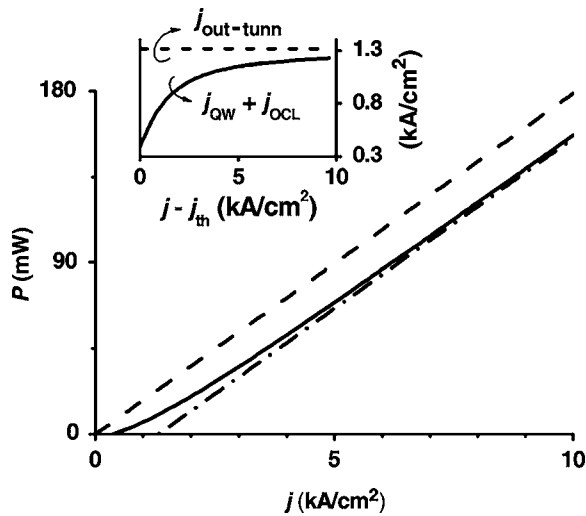


FIG. 2. LCC of a tunneling-injection QD laser (solid curve). The dashed line is the LCC of an ideal structure given by Eq. (8). The dash-dotted line is the asymptote given by Eq. (11). The inset shows the parasitic recombination current density (solid curve) and out-tunneling current density (horizontal dashed line) against excess injection current density. GaInAsP heterostructure lasing near $1.55 \mu\text{m}$ is considered here. The tunneling coefficients are as follows: $w_{p,\text{tunn}}^L = 0.073 \text{ cm}^2/\text{s}$, $w_{p,\text{tunn}}^R = 0.04 \text{ cm}^2/\text{s}$, $w_{n,\text{tunn}}^L = 0.013 \text{ cm}^2/\text{s}$, and $w_{n,\text{tunn}}^R = 0.058 \text{ cm}^2/\text{s}$.

In Eq. (9), $w_{p,\text{tunn}}^L N_S (1 - f_p) p_{QW}^L$ is the flux of backward tunneling of holes from the electron-injecting QW to QDs. By disregarding this flux, we get the upper limit for the parasitic recombination flux in the left-hand side of the structure. Since $f_{n,p} \ll 1$, this limit, which presents the out-tunneling flux $w_{p,\text{tunn}}^L p_1^{L,QW} N_S f_p$ of holes from QDs to the foreign (electron-injecting) QW, is itself restricted and cannot exceed $w_{p,\text{tunn}}^L p_1^{L,QW} N_S$ at any j . Consequently, the recombination flux in the left-hand-side QW and OCL is limited by $w_{p,\text{tunn}}^L p_1^{L,QW} N_S$,

$$B_{2D} n_{QW}^L p_{QW}^L + b_1 B_{nL} p_L < w_{p,\text{tunn}}^L p_1^{L,QW} N_S f_p < w_{p,\text{tunn}}^L p_1^{L,QW} N_S = \text{const.} \quad (10)$$

The parasitic recombination current density [the sum of the last four terms in the brackets in Eq. (7)] and the out-tunneling current density, $j_{\text{out-tunn}} = e w_{p,\text{tunn}}^L p_1^{L,QW} N_S f_p + e w_{n,\text{tunn}}^R n_1^{R,QW} N_S f_n$, are shown in the inset in Fig. 2 versus the excess injection current density, $j - j_{\text{th}}$.

By using Eq. (9) and a similar equation for the right-hand side of the structure, and by disregarding the current densities of the backward tunneling of minority carriers from the foreign QWs to QDs, we obtain from Eq. (7) the lower limit for the output power,

$$P^{\text{lowest}} = \frac{\hbar\omega}{e} S \left(j - e N_S \frac{f_n f_p}{\tau_{\text{QD}}} - e w_{p,\text{tunn}}^L p_1^{L,QW} N_S f_p - e w_{n,\text{tunn}}^R n_1^{R,QW} N_S f_n \right). \quad (11)$$

Since $f_{n,p} \ll 1$, the last three terms in the brackets in Eq. (11) remain restricted with increasing j .

As seen from Eq. (11), the lower limit for the LCC is linear (dash-dotted line in Fig. 2) and its slope efficiency is unity. It is parallel to the upper limit [given by Eq. (8) and

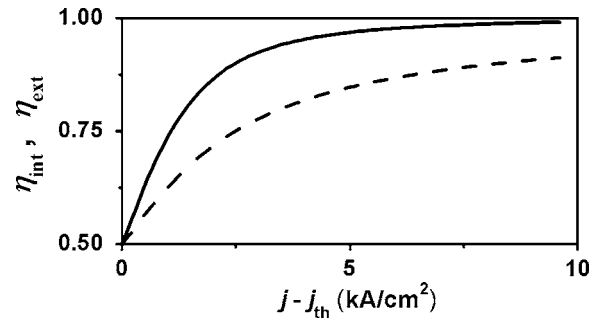


FIG. 3. Internal quantum efficiency $\eta_{\text{int}} = (eN/\tau_{\text{ph}})(1/S)/(j - j_{\text{th}})$ (dashed curve) and slope efficiency $\eta_{\text{ext}} = (e/\hbar\omega)(1/S)\partial P/\partial j$ (solid curve) against excess injection current density.

shown by the dashed line in Fig. 2] and shifted from the latter by the amount of the out-tunneling current density, $j_{\text{out-tunn}}$.

Hence, the actual LCC (obtained from the solution of the rate equations and shown by the solid curve in Fig. 2) is confined between the two parallel lines given by Eqs. (8) and (11) (dashed and dash-dotted lines in Fig. 2). Since the parasitic recombination current density (solid curve in the inset in Fig. 2) remains restricted, the fraction of the excess injection current density $j - j_{\text{th}}$ that goes into the stimulated emission [the internal quantum efficiency, $\eta_{\text{int}} = (eN/\tau_{\text{ph}})(1/S)/(j - j_{\text{th}})$] rises with increasing j (Fig. 3)—the LCC approaches the straight line given by Eq. (11) (Fig. 2).

In conclusion, we showed that the LCC of a laser exploiting tunneling-injection of both electrons and holes into QDs becomes more and more linear, and the slope efficiency grows closer to unity with increasing injection current. Such a feature is due to the fact that the current paths connecting the opposite sides of the structure lie entirely within QDs—in view of the three-dimensional confinement in QDs, the out-tunneling fluxes of carriers from dots (which are the source of parasitic recombination) are limited.

This work was supported by the U.S. Army Research Office under Grant No. W911-NF-05-1-0308.

- ¹L. V. Asryan, S. Luryi, and R. A. Suris, *Appl. Phys. Lett.* **81**, 2154 (2002).
- ²O. B. Shchekin, J. Ahn, and D. G. Deppe, *Electron. Lett.* **38**, 712 (2002).
- ³S. Fathpour, Z. Mi, and P. Bhattacharya, *Appl. Phys. Lett.* **85**, 5164 (2004).
- ⁴K. Kamath, D. Klotzkin, and P. Bhattacharya, Proceedings of the IEEE LEOS 10th Annual Meeting, 1997, Vol. 2, p. 498.
- ⁵P. Bhattacharya, X. Zhang, Y. Yuan, K. Kamath, D. Klotzkin, C. Caneau, and R. J. Bhat, *Proc. SPIE* **3283**, 702 (1998).
- ⁶P. Bhattacharya and S. Ghosh, *Appl. Phys. Lett.* **80**, 3482 (2002).
- ⁷H. C. Sun, L. Davis, S. Sethi, J. Singh, and P. Bhattacharya, *IEEE Photonics Technol. Lett.* **5**, 870 (1993).
- ⁸Y. Arakawa, *Solid-State Electron.* **37**, 523 (1994).
- ⁹L. V. Asryan and S. Luryi, *IEEE J. Quantum Electron.* **37**, 905 (2001).
- ¹⁰L. V. Asryan and S. Luryi, *Solid-State Electron.* **47**, 205 (2003).
- ¹¹L. V. Asryan and S. Luryi, U.S. Patent No. 6,870,178 (22 March 2005).
- ¹²T. Chung, G. Walter, and N. Holonyak, *Appl. Phys. Lett.* **79**, 4500 (2001).
- ¹³G. Walter, T. Chung, and N. Holonyak, *Appl. Phys. Lett.* **80**, 1126 (2002).
- ¹⁴G. Walter, T. Chung, and N. Holonyak, *Appl. Phys. Lett.* **80**, 3045 (2002).
- ¹⁵P. K. Kondratko, S.-L. Chuang, G. Walter, T. Chung, and N. Holonyak, *Appl. Phys. Lett.* **83**, 4818 (2003).
- ¹⁶S. L. Chuang and N. Holonyak, *Appl. Phys. Lett.* **80**, 1270 (2002).
- ¹⁷Z. Mi, P. Bhattacharya, and S. Fathpour, *Appl. Phys. Lett.* **86**, 153109 (2005).
- ¹⁸L. V. Asryan and R. A. Suris, *Semicond. Sci. Technol.* **11**, 554 (1996).